ARTICLES

Further Evidence of an Inverted Region in Proton Transfer within the Benzophenone/Substituted Aniline Contact Radical Ion Pairs; Importance of Vibrational Reorganization Energy

Libby R. Heeb and Kevin S. Peters*

Department of Chemistry and Biochemistry, University of Colorado, Boulder, Colorado 80309

Received: October 27, 2005; In Final Form: March 15, 2006

The dynamics of proton transfer within the triplet contact radical ion pair of a variety of substituted benzophenones with *N*,*N*-diethylaniline, *N*,*N*-dimethyl-*p*-toluinide, and *N*,*N*-diallylaniline are examined in solvents of varying polarity. The correlation of the rate constants with driving force reveal both a normal region and an inverted region providing support for the nonadiabatic nature of proton transfer within these systems. The reorganization of both the solvent and the molecular framework are central in governing the overall reaction dynamics.

Introduction

Since proton transfer is a fundamental process in both chemistry and biochemistry, understanding the factors that mediate its rate has been an important goal, and accordingly, proton-transfer reactions have been studied by both experimentalists and theorists for more than 60 years.[1−15] Our research group has been studying the proton-transfer reaction of the π-stacked benzophenone/*N*,*N*-dimethylaniline triplet contact radical ion pairs (CRIP) with the goal of comparing experimental results to the predictions of the newly developed Lee−Hynes model for proton transfer.[16−21] This model contrasts with the traditional transition state theory treatment that assumes the reaction path proceeds by thermal excitation over the reaction barrier in the proton-transfer coordinate with the possibililty of tunneling very near to the transition state accounted for by a Bell correction.[9] Central to the Lee−Hynes treatment is if an electronic barrier is encountered in the proton transfer coordinate, the proton tunnels through the barrier into product state. In order for tunneling to occur, the product and reactant state must be brought into resonance by solvent reorganization, which is a thermally activated event and accounts for the temperature dependence of the process. As with Marcus theory for electron transfer, under the appropriate conditions both a normal region and an inverted region may be manifested in the correlation of the rate constant for proton transfer with driving force; this behavior is not found in the classical transition state theory treatment. Indeed, in our previous work, clear inverted regions for these proton-transfer reactions were observed.[20] The position of the inverted region was shown to depend strongly on solvent as would be expected with a solvent-mediated process. In addition, a set of reasonable molecular parameters gave a good fit of the data to the Lee−Hynes model assuming that only zero-point vibrations in the reactant and product states were active.

In a recent theoretical study, Kiefer and Hynes examined the effects of tunneling between different vibrational levels of the reactant and the product states within the context of the kinetic deuterium isotope effect.[22] Assuming a linear geometry between the two heavy atoms and the transferring proton, transitions out of the reactant ground-state vibration into excited vibrations in the product state make a significant contribution to the overall reaction rate. In the product state, associated with an increase in vibrational quanta is an increase in vibrational amplitude that reduces the distance for tunneling. Thus, the tunneling rate constant for the 0 to 1 vibrational transition is larger than the tunneling rate constant for the 0 to 0 vibrational transition. The impact of participation of vibrational excitation in the product state for proton transfer is that as the driving force increases, the rate of proton-transfer continues to increase; an inverted region is not observed within this model for a linear configuration.

Contrary to these theoretical predictions, our studies and those of Saveant reveal an inverted region in proton-transfer reactions.[20,23] As mentioned previously, we have observed an inverted region in proton transfer within the contact radical ion pairs of substituted benzophenone/*N*,*N*-dimethylaniline as well as substituted benzophenone/*N*-methylacridan.[20,21] In our last study, we speculated that the deviation from the theoretical predictions can be rationalized by the difference in geometries; our systems are assumed to be π-stacked leading to nonlinear proton transfer between the two heavy atoms while the theoretical model of Kiefer and Hynes assumes a linear configuration. However, the Saveant group has studied proton transfer from a wide range of alcohols to the diphenylmethyl anion.[23] Since most of the alcohols studied will not π-stack with the diphenylmethyl anion, the transferring system should be linear, yet they observe a deep inverted region; the fastest rate constant is 80 times higher than the slowest rate constant at high driving forces. These experimental results have not yet been reconciled with the theory.[22]

The present investigation was undertaken for two purposes. First, in the previous studies, there was a concern that the CRIP energy was within a few kcal/mol of the benzophenone triplet

10.1021/jp056188w CCC: $33.50
Published on Web 04/29/2006

state energy.[20] As substituents on the benzophenone were varied to change the energy of the CRIP, an increase in the CRIP energy may lead to an increase in mixing between the CRIP and triplet states resulting in a change in the nature of the electronic structure of the radical anion of benzophenone. The proton transfer rate could then be artificially slowed with an increase in mixing; this may lead to the appearance of an inverted region because the CRIP energy is closer to the triplet state energy at higher driving forces. Thus, in the present study *N*,*N*-dimethylaniline is replaced by *N*,*N*-diethylaniline and by *N*,*N*-dimethyl-*p*-toluinide resulting in a stabilization of the CRIP on the order of 5 kcal/mol relative to the triplet state which should greatly reduce any potential problems of state mixing. Second, to further investigate the energy dependence of the inverted region, the driving force for proton transfer is extended by 10 kcal/mol by replacing *N*,*N*-dimethylaniline with *N*,*N*-diallylaniline.

Experimental Section

Reactions were studied in six different solvents: tetrahydrofuran (99.9%), 1,2-dichloroethane (100.0%), acetonitrile (99.93%), propionitrile (99%), butyronitrile (99+%), and valeronitrile (99.5%). All solvents except the 1,2-dichloroethane were purchased from Aldrich; the 1,2-dichloroethane was purchased from Mallinckrodt. All solvents were used as received. *N*,*N*-dimethyl-*p*-toluinide (Me−DMA) and *N*,*N*-diethylaniline (DEA) were purchased from Aldrich and were 99% and 99+% purity, respectively. The *N*,*N*-diallylaniline (DAA) was purchased from Pfaltz & Bauer and was 98+% purity. The eight different substituted benzophenone compounds employed were obtained from Aldrich: 4,4′-dimethoxybenzophenone (97%); 4,4′-dimethylbenzophenone (99%); 4-methoxybenzophenone (97%); 4-methylbenzophenone (99%); benzophenone (99%); 4-fluorobenzophenone (97%); 4-chlorobenzophenone (99%); 4,4′-dichlorobenzophenone (99%).

Picosecond absorption kinetics were measured using a picosecond laser system, described previously, employing a Continuum PY61C-10 laser with 8 ps pulses.[24] The samples were irradiated at 355 nm and the resulting dynamics probed at 680 nm. The sample was kept at room temperature, 23 °C, in a 1 cm path length quartz cuvette with a magnetic stir bar. Samples contained 0.02 M benzophenone and 0.4 M aniline derivative.

In fitting the theoretical model of Lee−Hynes to the correlation of the experimental rate constants with driving force, the vibrational frequencies associated with the transferring proton in the reactant state and product state were determined through electronic structure calculations as was the vibrational reorganization energy. The calculations were performed with MacSparatan Pro using the DFT model with the B3LYP 6-31G* basis set for the vibrational reorganization energies and at the AM1 level for the vibrational frequencies. The derived values for the vibrational frequencies were scaled by a factor of 0.9.[25]

Results and Discussion

Kinetic Scheme. The photochemistry of the processes leading up to proton transfer within the triplet contact radical ion pair has been well characterized for benzophenone and *N*,*N*-dimethylaniline (DMA).[16] The 355 nm excitation of benzophenone leads to the creation of the first excited singlet state, ^{1}Bp*, which decays to the first excited triplet state, ^{3}Bp*, on a time scale of less than 10 ps. The triplet state has an absorption maximum at λ_{max} 525 nm. An electron transfer from DMA to ^{3}Bp*, k_{et}, leads to the formation of the triplet contact radical ion pair (CRIP) consisting of the radical anion of benzophenone,

SCHEME 1

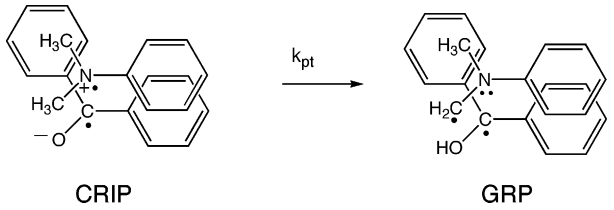

SCHEME 2

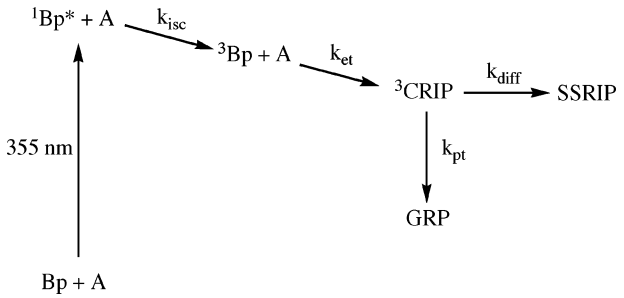

with λ_{max} = 710 nm, and the radical cation of DMA, with λ_{max} = 460 nm.[20] To prevent the formation of singlet CRIP, the amine concentrations were set at 0.4 M; it has previously been shown that amine concentrations greater than 0.8 M leads to electron transfer from the amine to ^{1}Bp* producing singlet CRIP.[16] The triplet CRIP decays by to two pathways on the picosecond time scale: through proton transfer, k_{pt}, producing the triplet geminate radical pair (GRP), and through diffusional separation to form the solvent separated radical ion pair (SSRIP), k_{dif}. Proton transfer within the triplet CRIP is assumed to occur in a π-stacked complex, Scheme 1. During the 1 ns time scale on which these molecular events occur, evolution of the triplet CRIP into the singlet CRIP has been shown not to intervene.[26,27]

A summary of the kinetic processes is shown in Scheme 2.

Kinetic Data. The formation and decay of the triplet contact radical ion pair for the various benzophenones with DEA, Me−DMA, and DAA were monitored at 680 nm and probed out to 1.5 ns. The kinetic data was fit to Scheme 2, varying three rate constants: k_{pt}, k_{dif}, and k_{et}. The method for data analysis has been discussed in detail previously.[16] An example of the fit of the model to the experimental data is shown in Figure 1. The formation of the CRIPs occurs with rate constants (k_{et}) greater than 10^{10} s^{-1}, substantially faster than the ensuing decays of the various CRIPs. The rate constant for proton transfer, k_{pt}, was found to vary over 1 order of magnitude ranging between 1×10^8 and 7×10^9 s^{-1}. The rate constants for diffusional separation, k_{dif}, varied between 4.5×10^6 and 9×10^8 s^{-1}. Table 1S gives the proton-transfer rate constants for all of the fits of the kinetic data collected as well as the rate constants for the DMA data collected previously.[21] The estimated error for k_{pt} is ± 10%.

Energetic Analysis. The driving force for the proton-transfer reaction, ΔG, is dependent on the energy of the CRIP and the energy of the geminate radical pair (GRP). The energy of the CRIP was calculated using the oxidation potential of DMA, E_D^{OX}, and the reduction potential of benzophenone, E_A^{RED}, both previously obtained through experiment, using the following formalism:

$$\Delta G_{CRIP} = (E_D^{OX} - E_A^{RED}) + \Delta_{CRIP} \quad (1)$$

where Δ_{CRIP} is a solvent correction based on the Onsager dipole model.[28] Some Δ_{CRIP} values were obtained from the literature

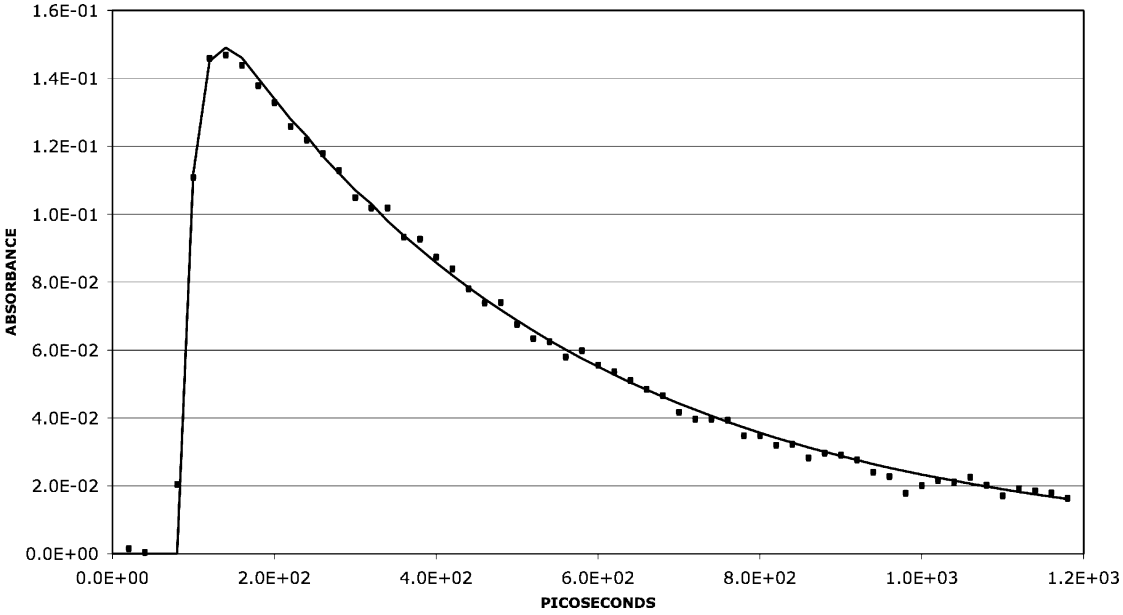

Figure 1. Transient absorption at 680 nm following the 355 nm excitation of 0.02 M *p*,*p*′-dimethoxybenzophenone in the presence of 0.4 M *N*,*N*-dimethyl-*p*-toluinide in 1,2 dichloroethane. Experimental data- squares. Fit (solid line) $k_{PT} = 2.26 \times 10^9\ s^{-1}$, $k_{dif} = 2.78 \times 10^7\ s^{-1}$, pulse width 9 ps, and $t_o = 93$ ps.

TABLE 1: Solvent Reorganization Energies, E_S, and Electronic Barrier Heights, $V^{\ddagger}$, Based upon the Fit of the Lee−Hynes Model to the Correlation of the Rate Constant for Proton Transfer with Driving Force for Benzophenone/*N*,*N*-Dimethylaniline (DMA), Benzophenone/*N*,*N*-Dimethyl-*p*-toluinide (Me−DMA), Benzophenone/*N*,*N*-Diethylaniline, and Benzophenone/*N*,*N*-Diallylaniline (DAA) CRIPs as a Function of Solvent

DMA	$V^{\ddagger}$ (kcal/mol)	E_s (kcal/mol)
THF	20.1	7.3
1,2-dichloroethane	20.8	7.5
acetonitrile	19.8	16.0
propionitrile	20.4	11.5
butyronitrile	20.6	9.0
valeronitrile	20.6	8.2
Me−DMA	**$V^{\ddagger}$ (kcal/mol)**	**E_s (kcal/mol)**
THF	20.4	9.7
1,2-dichloroethane	21.2	10.5
propionitrile	20.9	12.1
butyronitrile	20.9	12.1
valeronitrile	20.9	12.1
DEA	**$V^{\ddagger}$ (kcal/mol)**	**E_s (kcal/mol)**
THF	21.4	8.6
1,2-dichloroethane	22.0	8.5
acetonitrile	22.8	13.2
propionitrile	22.2	11.8
butyronitrile	22.1	11.3
valeronitrile	22.1	11.3
DAA	**$V^{\ddagger}$ (kcal/mol)**	**E_s (kcal/mol)**
THF	21.2	16.0
1,2-dichloroethane	21.6	18.1
acetonitrile	21.5	21.1
propionitrile	21.4	19.4
butyronitrile	21.4	17.8
valeronitrile	21.6	17.8

while others were obtained through extrapolation by correlating the experimental Δ_{CRIP} with E_T[30] values.[20,28] To obtain E_D^{OX} energies for Me−DMA, DEA, and DAA, the energy difference between each neutral aniline molecule and its corresponding radical cation was calculated via density functional theory (B3LYP 6−31*G basis set) which was then combined with the

SCHEME 3

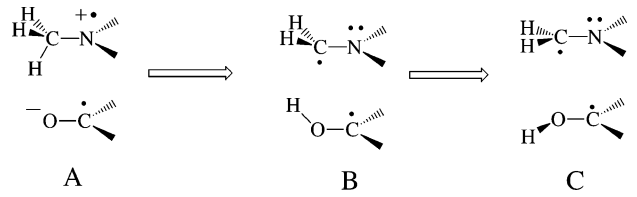

experimentally determined value E_D^{OX} for DMA.[29] Table 2S gives the results of these calculations. It should be noted that both DEA and DAA have a variety of possible orientations for their *N*-ethyl and N-allyl groups, respectively. These calculations were performed on several different conformations for each molecule. For both molecules, the most stable neutral was also the most stable radical cation, so only the most stable conformation was used.

To establish the energy of the radical pair for the product state, the geometry of the radical pair must be taken into account. In the π-stacked complex, the shortest distance for proton tunneling involves the creation of the radical pair in the conformation depicted as B in Scheme 3 where the O−H is aligned with the p-orbital of the carbon centered radical.[20] This positioning of the O−H bond corresponds to the transition state for O−H rotational coordinate. Thus, upon its formation, B would relax by a 90° rotation to conformation C in Scheme 3. Electronic structure calculations reveal that conformation B is 3.4 kcal/mol higher in energy than conformation C.[21]

The energy of the GRP was determined by adding the enthalpy of formation for the triplet state of benzophenone (62.9 kcal/mol), the enthalpy for addition of a hydrogen atom to the triplet state of benzophenone (−110.8 kcal/mol), and literature values for C−H bond dissociation enthalpy (H−BDE) for each of the respective anilines.[20,30,31] This sum represents the energy of the GRP associated with conformation C, Scheme 2. Since conformation B is the product state for proton transfer, an additional 3.4 kcal/mol is added to the energy of the GRP. The final radical pair energy is then given by (62.9−110.8 + H−BDE +3.4) kcal/mol. Table 3S lists the C−H bond dissociation and radical pair energies.

For the correlation of the rate constant for proton transfer with driving force, the free energy change for the process is employed. In the calculation of the energy of the CRIP relative to the initial reactants, the energy obtained relates to a free energy as the derived values are based upon electrochemical oxidation and reduction potentials. However, the thermodynamic cycles utilized in the determination of the energy of the GRP are based upon enthalpy changes. The entropy change associated with spin statistics of going from ground-state reactants to the triplet GRP is R ln 3, which at room temperature, contributes less than 1 kcal/mol and thus is neglected. The entropy differences for the molecular structures associated with the reactants and the GRP are assumed to be negligible.

Finally, benzophenone substituent effects upon the energy of the CRIP and the GRP are taken into account as the substituents effect both the energy of the benzophenone radical anion and the ketyl radical to differing degrees. These corrections have been discussed previously and are listed for both the CRIP and the GRP in, Table 4S.[20] Subtracting the CRIP energy from the GRP energy yields the driving force for the proton-transfer reaction, Table 5S.

In our last study of proton transfer within benzophenone/*N*,*N*-dimethylaniline triplet contact radical ion pair, there was concern that the source of the observed inverted region was due to a change in the electronic structure of the triplet contact radical ion pair resulting from the mixing with the triplet state of benzophenone.[20] As electron-donating substituents are added to benzophenone, the energy of the triplet contact radical ion pair increases. For example, replacing the hydrogens by *p*-dimethoxy substituents raises the energy of the contact radical ion pair from 64.9 to 69.2 kcal/mol in THF; the energy of the corresponding two triplet state are 69.2 and 69.9 kcal/mol. With this energy difference of less than 1 kcal/mol, there could be substantial mixing of the contact radical ion pair state and the triplet state of the dimethoxy-system that is not present in the unsubstituted system. However, picosecond absorption spectra of the reacting contact radical ion pair revealed no evidence of such mixing and it was concluded that the procedure for determining the energy of the contact radical ion pair overestimates its value. With the present molecular systems, the energy of the contact radical ion pairs is reduced by 5 kcal/mol for Me−DMA, 4.1 kcal/mol for DEA, and 4.5 kcal/mol for DAA relative to DMA. If all of the systems manifest consistent kinetic behavior in relation to the inverted region, the source of the effect cannot be attributed to state mixing.

Lee—Hynes Model. In 1993, Azzouz and Borgis calculated that tunneling is 1000 times faster than thermal excitation over the reaction barrier for linear nonadiabatic proton-transfer reactions in the model system [OH−N] to [O−HN].[32] The Lee−Hynes model describes this proton tunneling process; it allows for more than one vibrationally active state in both the reactant and product states, an improvement upon an earlier version of the model.[9] The Lee−Hynes model defines the rate constant for nonadiabatic proton transfer from the *n*th vibrational level of the reactant state to the *m*th vibrational level of the product state as follows:

$$k(n_r \rightarrow m_p) = k_{m_p,n_r}(0)(\pi/2A_2)^{1/2} \exp(-A_1^2/2A_2) \quad (2)$$

where $k_{m_p,n_r}(0)$, A_1, and A_2 are defined as

$$k_{m_p,n_r}(0) = 2(2\pi/h)^2[C_{m_p,n_r}(Q)]^2 \exp\{(E_\alpha/h\omega_Q) \times 2 \coth(\beta h\omega_Q/2)\} \quad (3)$$

$$A_1 = (2\pi/h)\{\Delta E + E_S + E_Q + E_\alpha + [hm_P\omega_P - hm_R\omega_R] + 2\Delta Q/|Q|(E_\alpha E_Q)^{1/2} * \coth(\beta h\omega_Q/2)\} \quad (4)$$

$$A_2 = 2(2\pi/h)^2 k_B T\{E_S + (E_Q + E_\alpha)(\beta h\omega_Q/2\pi\coth(\beta h\omega_Q/2\pi)) + \Delta Q/|\Delta Q|(E_\alpha E_Q)^{1/2}\beta h\omega_Q\} \quad (5)$$

In the above expressions, ω_R and ω_P are vibrational frequencies for the n_R level of the reacting proton stretch and the m_P level of the product proton stretch. These frequencies were determined by AM1 calculations to be 2716 cm^{-1}, 2719, 2689, and 2684 cm^{-1} for DMA, Me−DMA, DEA, and DAA, respectively. The ω_Q is a low-frequency normal mode vibration associated with the intermolecular separation between CRIP anion and cation; this term is unique to the models developed by Hynes and coworkers. E_s is the solvent reorganization energy. ΔQ is the change in equilibrium distance between the reactant and product; the energy associated with this change is E_s. Since the magnitude of ΔQ is unknown, its value is set to zero with the result that $E_Q = 0$. ΔE is the driving force for the reaction. $C_{m_p,n_r}(Q)$ is the tunneling matrix element from the *n*th level of the reactant to the *m*th level of the product. It is given by

$$C_{m_p,n_r}(Q) = (h/4\pi^2)(\omega_R\omega_P)^{1/2} \exp\{(-2\pi^2/h\omega^\ddagger)[V^\ddagger - {}^1/_2(V_{n_R} + V_{m_P})]\} \quad (6)$$

where $\omega^\ddagger$ is a mass-weighted imaginary frequency associated with the inverted parabola of the transition state in the proton-transfer coordinate, $V^\ddagger$ is the barrier height, and V_{nr} and V_{mp} are the reactant (CRIP) and product (GRP) state energies, calculated previously. The parameter α is a purely quantum length term that describes the distance dependence of the wave function overlap. The energy term E_α is the energy related to this length, given by

$$E_\alpha = h^2\alpha^2/2m \quad (7)$$

and is estimated to be approximately 1.0 kcal/mol.[3]

The development of both a normal region and an inverted region in the correlation of the rate constant for proton transfer with driving force is governed by the term A_1 in eq 4. A depiction for the solvent dependence of the proton-transfer coordinate as a function of driving force ΔE is shown in Figure 2 and is applicable only to the situation in which the proton tunnels out the of ground vibrational state of the reactant and into the ground vibrational state of the product. When the driving force $\Delta E = 0$, the system is in normal regime for proton transfer. In this regime at the solvent coordinate S_R, the product state is higher in energy than the reactant state. A fluctuation in the solvent coordinate from S_R to S_{TS} brings the two states into resonance allowing the proton to tunnel into the product state. When the driving force is of the same magnitude as the total reorganization energy, $|\Delta E| = \lambda$, there is no requirement for solvent reorganization as the reactant and product states are in the resonance required for tunneling at the solvent configuration S_R which has the same configuration as S_{TS}; this corresponds to the maximum rate for proton transfer. Finally, when $|\Delta E| > \lambda$, a fluctuation in the solvent coordinate from S_R to S_{TS} is again required to bring the two states into resonance for proton tunneling. In this regime, as magnitude of $|\Delta E|$ increases the

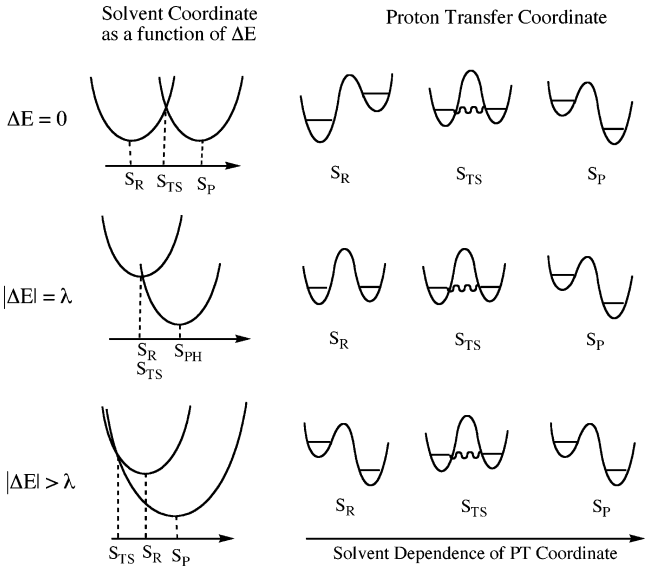

Figure 2. Pictorial representation for the dependence of the proton-transfer coordinate on the solvent coordinate as a function of driving force, ΔE. The solvent configuration for the reactant state is S_R, for the product state is S_P, and for the transition state is S_{TS}. $\lambda = E_S + E_\alpha$ assuming $\Delta Q = 0$ and $E_Q = 0$ in eq 4.

rate of proton transfer will decrease, placing the system into the inverted regime.

Fit of Lee—Hynes Model to Experiment. Examining the correlation of the rate constants for proton transfer with driving force within the context of the Lee−Hynes model requires an assumption regarding which vibrations of the product state will be active. In our previous study, allowing for the participation of the zero point vibrations for both the O−H bending and stretching modes to be active gave a superior fit to the experimental data when compared to having only the O−H stretching mode and its overtones active.[20] The rational for this assumption is based upon the rather unique structure of the product state B, Scheme 3. The overtones in either the O−H stretch or bends lead to a larger distance for proton tunneling relative to the zero point vibrations; thus only the zero point vibrations are assumed to be active. It should be noted that this would not be the case for a linear arrangement for the hydrogen bond.

For this study, the parameters that serve as variables in the Lee−Hynes model fitting are the barrier height $V^\ddagger$ and the solvent reorganization energy E_S; the values of the remaining parameters are held constant and are given in the figure captions. The choice for the values of these parameters is discussed in our earlier work.[20] The fit of the model to the experiments for the four amines in THF are shown in Figure 3 where each set of data reveals both a normal and an inverted region in the correlation of the rate constant with driving force. The position of the maximum rate with respect to driving force is mainly determined by the solvent reorganization energy E_S. In THF, the value of E_S is 7.3 kcal/mol for DMA, 8.6 kcal/mol for DEA, 9.7 kcal/mol for Me−DMA, and 16.0 kcal/mol for DAA. The values for the barrier height are similar for the four amines ranging from 20.1 to 21.4 kcal/mol. An increase in the barrier height of 1.3 kcal/mol leads to a reduction in the rate constant for proton transfer by a factor of 3.5. Similar behavior is found for the solvent 1,2-dichloroethane, Figure 4, where there is a small increase E_S for each of the amines relative to values in THF. The trend of increasing E_S with increasing solvent polarity can also be found for the solvents butyronitrile, Figure 5, and propionitrile, Figure 6. The values of $V^\ddagger$ and E_S for each of the amines in the various solvents are given in Table 1.

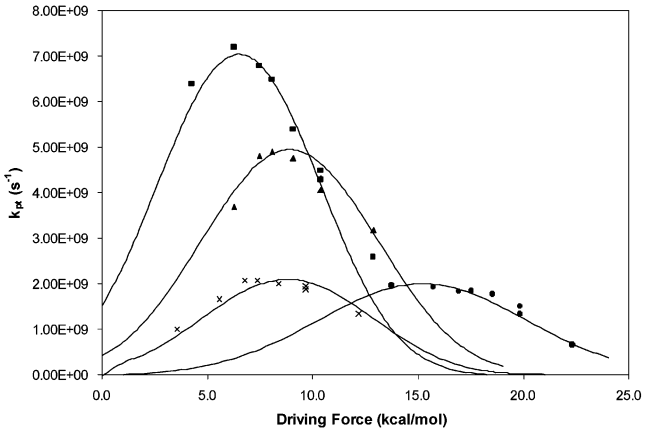

Figure 3. Plot of the experimental rate constant for proton transfer vs negative free energy change (driving force, kcal/mol) for the solvent tetrahydrofuran. Experimental data: benzophenone/*N*,*N*-dimethylaniline (squares), benzophenone/*N*,*N*-dimethyl-*p*-toluinide (triangles), benzophenone/*N*,*N*-diethylaniline (×'s), and benzophenone/*N*,*N*-diallylaniline (circles). Solid curve fits based on the Lee−Hynes model with $E_\alpha = 1.0$ kcal/mol, $\omega_Q = 200$ cm^{-1}, $\Delta Q = 0$, $E_Q = 0$ kcal/mol, $\omega_R = 2701$ cm^{-1}, and $\omega^\ddagger = 2500$ cm^{-1} held constant. Key: benzophenone/*N*,*N*-dimethylaniline (squares), $V^\ddagger = 20.1$ kcal/mol, $E_S = 7.3$ kcal/mol, $\omega_P = 2716$ cm^{-1} stretch and 768 cm^{-1} bend; benzophenone/*N*,*N*-dimethyl-*p*-toluinide (triangles), $V^\ddagger = 20.4$ kcal/mol, $E_S = 9.7$ kcal/mol, $\omega_P = 2719$ cm^{-1} stretch and 768 cm^{-1} bend; benzophenone/*N*,*N*-diethylaniline (×'s), $V^\ddagger = 21.4$ kcal/mol, $E_S = 8.6$ kcal/mol, $\omega_P = 2689$ cm^{-1} stretch and 768 cm^{-1} bend; benzophenone/*N*,*N*-diallylaniline (circles), $V^\ddagger = 21.2$ kcal/mol, $E_S = 16.0$ kcal/mol, $\omega_P = 2684$ cm^{-1} stretch and 768 cm^{-1} bend.

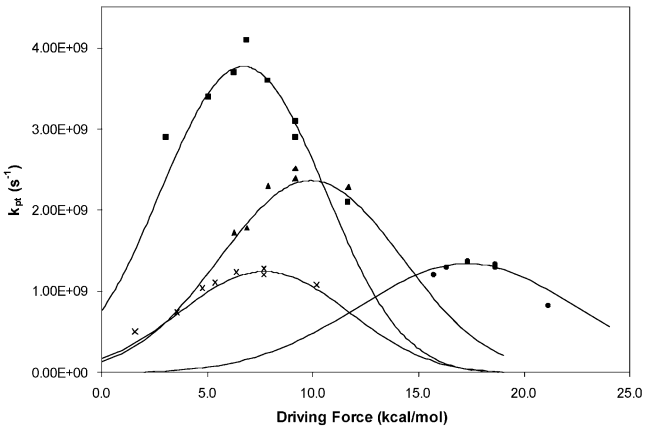

Figure 4. Plot of the experimental rate constant for proton transfer vs negative free energy change (driving force, kcal/mol) for the solvent 1,2 dichlorethane. Experimental data: benzophenone/*N*,*N*-dimethylaniline (squares), benzophenone/*N*,*N*-dimethyl-*p*-toluinide (triangles), benzophenone/*N*,*N*-diethylaniline (×'s), and benzophenone/*N*,*N*-diallylaniline (circles). Solid curve fits based on the Lee−Hynes model with $E_\alpha = 1.0$ kcal/mol, $\omega_Q = 200$ cm^{-1}, $\Delta Q = 0$, $E_Q = 0$ kcal/mol, $\omega_R = 2701$ cm^{-1}, and $\omega^\ddagger = 2500$ cm^{-1} held constant. Key: benzophenone/*N*,*N*-dimethylaniline (squares), $V^\ddagger = 20.8$ kcal/mol, $E_S = 7.5$ kcal/mol, $\omega_P = 2716$ cm^{-1} stretch and 768 cm^{-1} bend; benzophenone/*N*,*N*-dimethyl-*p*-toluinide (triangles), $V^\ddagger = 21.2$ kcal/mol, $E_S = 10.5$ kcal/mol, $\omega_P = 2719$ cm^{-1} stretch and 768 cm^{-1} bend; benzophenone/*N*,*N*-diethylaniline (×'s), $V^\ddagger = 22.0$ kcal/mol, $E_S = 8.5$ kcal/mol, $\omega_P = 2689$ cm^{-1} stretch and 768 cm^{-1} bend; benzophenone/*N*,*N*-diallylaniline (circles), $V^\ddagger = 21.6$ kcal/mol, $E_S = 18.1$ kcal/mol, $\omega_P = 2684$ cm^{-1} stretch and 768 cm^{-1} bend.

Variation of E_S with Amine. A feature of note found in Figures 3-6 is dependence of the peak position on the amine. In Lee−Hynes theory, the position of the peak maximum is determined by solvent reorganization energy, E_S. Given that the

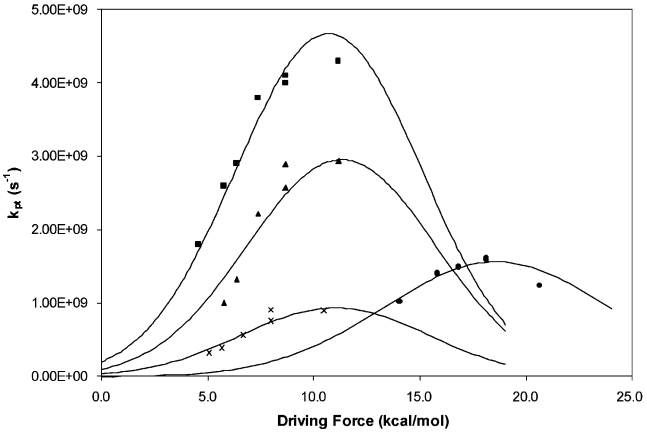

Figure 5. Plot of the experimental rate constant for proton transfer vs negative free energy change (driving force, kcal/mol) for the solvent propionitrile. Experimental data: benzophenone/*N*,*N*-dimethylaniline (squares), benzophenone/*N*,*N*-dimethyl-*p*-toluinide (triangles), benzophenone/*N*,*N*-diethylaniline (×'s), and benzophenone/*N*,*N*-diallylaniline (circles). Solid curve fits based on the Lee−Hynes model with $E_\alpha = 1.0$ kcal/mol, $\omega_Q = 200$ cm^{-1}, $\Delta Q = 0$, $E_Q = 0$ kcal/mol, $\omega_R = 2701$ cm^{-1}, and $\omega^\ddagger = 2500$ cm^{-1} held constant. Key: benzophenone/*N*,*N*-dimethylaniline (squares), $V^\ddagger = 20.4$ kcal/mol, $E_S = 11.5$ kcal/mol, $\omega_P = 2716$ cm^{-1} stretch and 768 cm^{-1} bend; benzophenone/*N*,*N*-dimethyl-*p*-toluinide (triangles), $V^\ddagger = 20.9$ kcal/mol, $E_S = 12.1$ kcal/mol, $\omega_P = 2719$ cm^{-1} stretch and 768 cm^{-1} bend; benzophenone/*N*,*N*-diethylaniline (×'s), $V^\ddagger = 22.2$ kcal/mol, $E_S = 11.8$ kcal/mol, $\omega_P = 2689$ cm^{-1} stretch and 768 cm^{-1} bend; benzophenone/*N*,*N*-diallylaniline (circles), $V^\ddagger = 21.4$ kcal/mol, $E_S = 19.4$ kcal/mol, $\omega_P = 2684$ cm^{-1} stretch and 768 cm^{-1} bend.

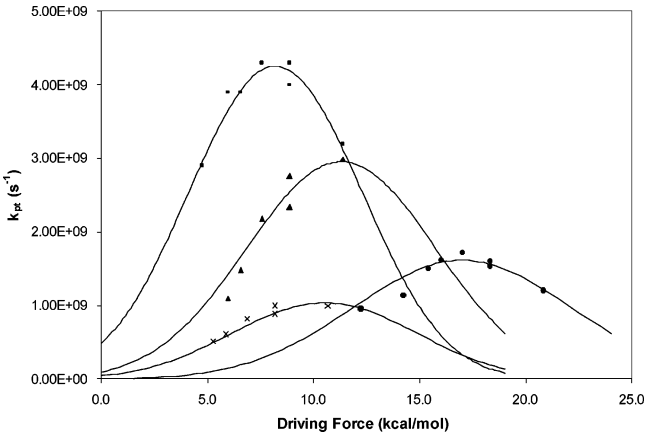

Figure 6. Plot of the experimental rate constant for proton transfer vs negative free energy change (driving force, kcal/mol) for the solvent butyronitrile. Experimental data: benzophenone/*N*,*N*-dimethylaniline (squares), benzophenone/*N*,*N*-dimethyl-*p*-toluinide (triangles), benzophenone/*N*,*N*-diethylaniline (×'s), and benzophenone/*N*,*N*-diallylaniline (circles). Solid curve fits based on the Lee−Hynes model with $E_\alpha = 1.0$ kcal/mol, $\omega_Q = 200$ cm^{-1}, $\Delta Q = 0$, $E_Q = 0$ kcal/mol, $\omega_R = 2701$ cm^{-1}, and $\omega^\ddagger = 2500$ cm^{-1} held constant. Key: benzophenone/*N*,*N*-dimethylaniline (squares), $V^\ddagger = 20.6$ kcal/mol, $E_S = 9.0$ kcal/mol, $\omega_P = 2716$ cm^{-1} stretch and 768 cm^{-1} bend; benzophenone/*N*,*N*-dimethyl-*p*-toluinide (triangles), $V^\ddagger = 20.9$ kcal/mol, $E_S = 12.1$ kcal/mol, $\omega_P = 2719$ cm^{-1} stretch and 768 cm^{-1} bend; benzophenone/*N*,*N*-diethylaniline (×'s), $V^\ddagger = 22.1$ kcal/mol, $E_S = 11.3$ kcal/mol, $\omega_P = 2689$ cm^{-1} stretch and 768 cm^{-1} bend; benzophenone/*N*,*N*-diallylaniline (circles), $V^\ddagger = 21.4$ kcal/mol, $E_S = 17.8$ kcal/mol, $\omega_P = 2684$ cm^{-1} stretch and 768 cm^{-1} bend.

four amines are similar in structure in terms of size, it is anticipated that they should have similar solvent reorganization energies; thus the maximum in the correlation of rate constant with driving force should occur at similar values for the driving force. This is contrary to observation. In the development of proton-transfer model by Lee and Hynes, the contribution of energy associated with the vibrational reorganization, E_{VIB}, was not taken into account explicitly. As with electron transfer, it is the total reorganization energy, the combination of E_S and E_{VIB}, that will involved in determing the position of the peak maximum. Thus, based on eq 4, the maximum rate occurs when $A_1 = 0$ and is achieved when $|\Delta E| = (E_S + E_{VIB}) + E_\alpha$ assuming $\Delta Q = 0$ and $E_Q = 0$ for our system. Therefore, the original solvent reorganization energy parameter in Lee−Hynes model should reflect the combination of the solvent reorganization energy E_S and the vibrational reorganization energy E_{vib}. The difference in E_S of 8.7 kcal/mol for DMA and DAA in THF should the viewed as primarily as the difference in the vibrational reorganization energy between the two amines.

To gain insight into the magnitudes of the vibrational reorganization energies associated with the transfer of a proton from the amine radical cation to form the amine radical, electronic structure calculations were performed using DFT with a B3LYP 6-31G* basis set. First the geometry of the amine radical cation was optimized. From this geometry the energy of the radical was calculated by removing the transferring proton and holding the remaining atoms fixed. Then, the radical was allowed to relax and the energy of this equilibrium geometry was determined. The difference in energy between the equilibrated and nonequilibrated forms of the radical is an estimate of the vibrational reorganization energy. The procedure results in energies for vibrational reorganization of 9.8 kcal/mol for DMA, 10 kcal/mol for Me−DMA, 14 kcal/mol for DEA, and 27 kcal/mol for DAA. The difference in the calculated values for DMA and DAA, 17.2 kcal/mol, overestimates the observed difference of 8.7 kcal/mol by a factor of 2. This discrepancy is similar in magnitude to that found in the calculations of vibrational reorganization energies for electron transfer.[33]

The greatest source of error in the calculation of the vibrational reorganization energy is in the procedure of holding the atoms of the product radical fixed at the equilibrium geometry of the radical cation. In the reaction trajectory, there is a normal vibrational mode that will move the transferring proton toward the reaction barrier prior to tunneling. As the proton moves toward the barrier, the others atoms associated with the transferring mode will move in concert leading to a reorganization of the molecular structure of the radical cation toward that of the radical. The net effect of this motion is to reduce the vibrational reorganization energy relative to that estimated by holding the atoms in the radical fixed at the equilibrium geometry of the radical cation.

The initial motivation in examining the free energy dependence of proton transfer within the benzophenone/*N*,*N*-diallylaniline contact radical ion pair was the realization that this system provided an overall greater driving force by 10 kcal/mol when compared to *N*,*N*-dimethylaniline system. The expectation was that contributions of vibrational overtones in the product state would be manifested that were not revealed in the earlier studies of DMA. What was not anticipated was that the energy associated with the vibrational reorganization of DAA system is substantially larger than the DMA system, so that the peak maximum in the correlation of the rate of proton transfer with driving force moves to larger driving force by approximately 9 kcal/mol. The larger vibrational reorganization energy of DAA precludes the assessment of contributions of vibrational overtones in the product state to the overall kinetics of proton transfer.

Conclusions

The present study supports our previous conclusions regarding the nature of the proton-transfer process occurring in benzophe-

none/*N*,*N*-dimethylaniline contact radical ion pairs. The observation of both a normal and inverted region in the correlation of rate constants for proton transfer with driving force further substantiates the nonadiabatic nature of the process. Reorganization in both the solvent and vibrational coordinates is fundamental in governing the overall reaction dynamics. The standard model for proton-transfer based upon transition state theory, with the inclusion of tunneling in the region of the transfer state, cannot describe the kinetic behavior found in the current studies.

An issue that still remains to be addressed is the importance of a nonlinear geometry for manifestation of the inverted region. For a linear configuration, theory predicts that there should not be an inverted region as the tunneling factor increases with vibrational excitation in the product state. Yet, Saveant's studies of bimolecular proton transfer which presumably occur in a linear configuration, due to the lack of π-complex, also reveals an inverted region. The source of discrepancy between theory and experiment waits elucidation.[22,23]

Acknowledgment. This work is supported by a grant from the National Science Foundation, No. CHE-0408265. L.R.H. acknowledges support from University of Colorado OSEP, an NSF-IGERT program.

Supporting Information Available: Tables of rate constants for proton transfer, energies in kcal/mol for the triplet contact radical ion pairs, α-C−H bond dissociation energies, benzophenone substituent effects, and the driving force in kcal/mol for proton transfer. This material is available free of charge via the Internet at http://pubs.acs.org.

References and Notes

(1) Bell, R. P. *The Proton in Chemistry*; Chapman and Hall: London, 1973.
(2) Bell, R. P. *The Tunnel Effect in Chemistry*; Chapman and Hall: London, 1980.
(3) Borgis, D.; Hynes, J. T. *J. Phys. Chem.* **1996**, *100*, 1118.
(4) Kohen, A.; Klinman, J. P. *Acc. Chem. Res.* **1998**, *31*, 397.
(5) Kuznetsov, A. M. *Charge Transfer in Physics, Chemistry and Biology*; Gordon and Breach: Luxembourg, 1995.
(6) Morillo, M.; Cukier, R. I. *J. Chem. Phys.* **1990**, *92*, 4833.
(7) Hammes-Schiffer, S. *Acc. Chem. Res.* **2001**, *34*, 273.
(8) Li, D.; Voth, G. A. *J. Phys. Chem.* **1991**, *95*, 10425.
(9) Lee, S.; Hynes, J. T. *J. Chim. Phys.* **1996**, 1783.
(10) Barbara, P. F.; Walsh, P. K.; Brus, L. E. *J. Phys. Chem.* **1989**, *93*, 29.
(11) Pines, E.; Fleming, G. R. *J. Phys. Chem.* **1991**, *95*, 10448.
(12) Pines, E.; Fleming, G. R. *Chem. Phys.* **1994**, *183*, 393.
(13) Zewail, A. H. *J. Phys. Chem.* **1996**, *100*, 12701.
(14) Hineman, M. F.; Bruker, G. A.; Kelley, D. F.; Bernstein, E. R. *J. Chem. Phys.* **1990**, *92*, 805.
(15) Brucker, G. A.; Swinney, T. C.; Kelley, D. F. *J. Phys. Chem.* **1991**, *95*, 3190.
(16) Peters, K. S. *Advances in Photochemistry*; John Wiley & Sons: New York, 2002; Vol. 27.
(17) Peters, K. S.; Cashin, A. *J. Phys. Chem.* **2000**, *104*, 4833.
(18) Peters, K. S.; Cashin, A.; Timbers, P. J. *J. Am. Chem. Soc.* **2000**, *122*, 107.
(19) Peters, K. S.; Kim, G. *J. Phys. Chem.* **2001**, *105*, 4177.
(20) Peters, K. S.; Kim, G. *J. Phys. Chem. A* **2004**, *108*, 2598.
(21) Peters, K. S.; Kim, G. *J. Phys. Org. Chem.* **2004**, *17*, 1.
(22) Kiefer, P. M.; Hynes, J. T. *J. Phys. Chem. A* **2002**, *108*, 11793.
(23) Andrieux, C. P.; Gamby, J.; Hapiot, P.; Saveant, J. M. *J. Am. Chem. Soc.* **2003**, *125*, 10119.
(24) Peters, K. S.; Lee, J. J. *J. Phys. Chem.* **1992**, *96*, 8941.
(25) Hehre, W. J.; Yu, J.; Klunzinger, P. E.; Lou, L. *A Brief Guide to Molecular Mechanics and Quantum Chemical Calculations*; Wavefunction, Inc.: Irvine, CA, 1998.
(26) Peters, K. S.; Lee, J. *J. Phys. Chem.* **1993**, *97*, 3761.
(27) Miyasaka, H.; Morita, K.; Kamada, K.; Mataga, N. *Bull. Chem. Soc. Jpn.* **1990**, *63*, 3385.
(28) Arnold, B. R.; Farid, S.; Goodman, J. L.; Gould, I. R. *J. Am. Chem. Soc.* **1996**, *118*, 5482.
(29) Parker, V. D.; Tilset, M. *J. Am. Chem. Soc.* **1991**, *113*, 8778.
(30) Dombrowski, G. W.; Dinnocenzo, J. P.; Farid, S.; Goodman, J. L.; Gould, I. R. *J. Org. Chem.* **1999**, *64*, 427.
(31) Arnaut, L. G.; Caldwell, R. A. *J. Photochem. Photobiol. A: Chem.* **1992**, *65*, 15.
(32) Azzouz, H.; Borgis, D. *J. Chem. Phys.* **1993**, *98*, 7361.
(33) Nelsen, S. F.; Blomgren, F. *J. Org. Chem.* **2001**, *66*, 6551.